Electromagnetic Parameters of IPM Motors based on the Genetic Algorithm Technique

Quang Nguyen Duc
Faculty of Electrical Engineering, Electric Power University, Ha Noi, Vietnam
quangndhtd@epu.edu.vn

Thang Nguyen Duy
School of Electrical and Electronic Engineering, Hanoi University of Science and Technology, Vietnam
thang.nd210779@sis.hust.edu.vn

Trinh Truong Cong
School of Electrical and Electronic Engineering, Hanoi University of Science and Technology, Vietnam
trinh.truongcong@hust.edu.vn

Nam Le Hai
School of Electrical and Electronic Engineering, Hanoi University of Science and Technology, Vietnam
nam.lh210629@sis.hust.edu.vn

Duong Doan Le Quy
School of Electrical and Electronic Engineering, Hanoi University of Science and Technology, Vietnam
duong.dlq212493@sis.hust.edu.vn

Vuong Dang Quoc
School of Electrical and Electronic Engineering, Hanoi University of Science and Technology, Vietnam
vuong.dangquoc@hust.edu.vn

Dinh Bui Minh
School of Electrical and Electronic Engineering, Hanoi University of Science and Technology, Vietnam
dinh.buiminh@hust.edu.vn (corresponding author)

Received: 13 February 2025 | Revised: 21 March 2025 | Accepted: 2 April 2025

 DOI: https://doi.org/10.48084/etasr.10559

ABSTRACT

Interior Permanent Magnet Synchronous Motors (IPMSM) are increasingly utilized across various fields as a result of their superior performance and high power density. To ensure efficient operation in electric vehicles and industrial applications, these motors have to meet the stringent performance objectives of low vibration. This study proposes an optimization method based on Genetic Algorithm (GA) techniques to minimize losses and material costs. First, an analytical model is developed to determine the required parameters for an IPM motor with five pole pairs, 15 slots, and a power rating of 7.5 kW. Subsequently, the GA is implemented using the analytical model to optimize the electromagnetic parameters of the IPM motor. Finally, the Finite Element Method (FEM) is applied to simulate the parameters obtained from the analytical model and GA. The results before and after optimization, including material cost functions, total losses, and motor outputs, were compared to validate the proposed method.

Keywords-Interior Permanent Magnet Synchronous Motor (IPMSM); GA; cogging torque; torque ripple; analytical model

I. INTRODUCTION

Due to their high power density, efficiency, stable operation, and reliability, the Permanent Magnet Synchronous Motors (PMSMs) have been widely applied in industrial fields and electric vehicles in recent years [1-6]. PMSMs have contributed significantly to technological advancements and the creation of more energy-efficient systems by using permanent magnet materials such as neodymium-iron-boron (NdFeB) and samarium-cobalt (SmCo) [7]. In [8, 9], the Genetic Algorithm (GA) was used to optimize the main parameters of the motor. This technique has been employed in numerous studies to analyze optimal PMSM designs [10-13]. In [10], a multi-objective optimization design was developed for PMSMs using the artificial bee colony algorithm, achieving high dynamic performance and overall efficiency of 94.5% to 96%. In [11], a subdomain model was combined with GA to optimize the design of Surface-mounted PMSMs (SPMSMs). This study used a subdomain model to accurately evaluate the flux density harmonics. Next, a Pareto-optimal set of solutions was searched with the subdomain model, allowing time savings. Finally, the electromagnetic performance of the new design was verified using FEM and compared with the original design and the traditionally GA-optimized design. In [12], the GA technique was utilized in conjunction with Taguchi optimization and FEM to calculate the performance of SPMSMs. The results indicated that a reduction in the cogging torque results in a small reduction of efficiency from GAs to Taguchi design due to the reduction of magnet volume. In [13], an improved SPMSM design was proposed to reduce torque pulsations and save magnet costs. In [14, 15], a partitioned model was combined with GA to achieve an optimal SPMSM design. In this study, the partitioned model was developed in advance to accurately assess the flux density. Then, a Pareto-optimal set of solutions was obtained by applying the GA technique.

In this context, this study uses the GA technique to improve the electromagnetic parameters of IPM motors. First, an analytical model is provided to define the parameters required for motor design. Then, an optimization model based on the GA technique is developed to optimize the material cost and losses of the motor. Finally, FEM is applied to perform simulations and compare the results of the electromagnetic parameters of the proposed motor before and after optimization.

II. ANALYTICAL BACKGROUND

Figure 1 provides the analytical design steps of the PMSM. The volume (V_r) of the rotor is defined via the torque density (TRV) [16]:

$$V_r = \frac{\pi}{4}.{D_{is}}^2.L = \frac{T}{TRV} \quad (1)$$

where T is the electromagnetic torque, D_{is} is the inner diameter of the stator, and L is the length of the rotor.

The TRV value is selected from 35 kNm/m^3 to 85 kNm/m^3 [16]. The stator can be calculated similarly to the stator of an asynchronous motor, using the following formulas [16]:

$$D_{is} = \sqrt[3]{\frac{4V_r}{\pi.k_{shape}}} \quad (2)$$

where k_{shape} is the shape factor given in [16]. The thickness of the magnet is determined by:

$$d_m = \frac{\mu_r.geffB_g}{4B_r \sin(\alpha) - B_g\pi} \quad (3)$$

where B_r is the PM remanence, g_{eff} is the effective air gap length, μ_r is the relative permeability of the PM, and B_g is the magnetic flux density in the air gap. The B_g vallue can be selected from 0.8 T to 1.05 T [16]. The width of the magnet is determined by:

$$w_m = \frac{A_m}{L} \quad (4)$$

The PM opening angle in electrical degrees is computed as:

$$\beta = 2p.\arcsin\left[w_m.\left(\frac{\alpha_V}{D_{or}-2x_1}\right)\right] \quad (5)$$

The depth (d_p) of a V-shape pole (α_V) is given by:

$$d_p = x_1 + w_m.cos\left(\frac{\alpha_V}{2}\right) + \left(\frac{D_{or}}{2} - x_1\right)\left[1 - cos\left(\frac{\beta}{2}\right)\right] + \frac{d_m}{sin\left(\frac{\alpha_V}{2}\right)} \quad (6)$$

where w_m is the width of the PM. The height of the rotor yoke and the number of turns are represented below:

$$h_{ry} = \frac{\phi_g}{2.B_{ry}.L.k_j} - d_p;\ N_c = \frac{U_{phase}}{\pi\sqrt{2}fk_wB_gD_{ir}L} \quad (7)$$

The parameters h_{sy} and w_t have been already defined in [17]. The V-angle of the magnet and the magnitude of the bridge length in the IPM motor can also be adjusted depending on the design to suit the requirements.

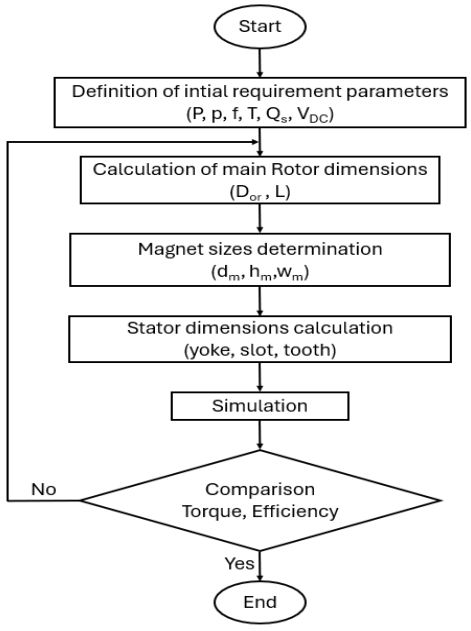

Fig. 1. Design steps of PMSM.

TABLE I. COMPUTATIONAL PARAMETERS OF THE 7.5KW IPM MOTOR

Parameters	Values	Unit
Number of slots	15	
Number of poles	10	
Inner diameter of stator	151.45	mm
Outer diameter of stator	240.53	mm
Tooth width	14.46	mm
Slot height	30.6	mm
Air gap length	0.8	mm
Inner diameter of rotor	108.77	mm
Magnet thickness	2.3	mm
Magnet width	20.4	mm
Bridge length	2	mm
V-angle	114	Elec degrees
Electrical angle of the magnet	149.3	Elec degrees
Number of turns	29	

III. GA TECHNIQUE FOR PARAMETER OPTIMIZATION

GA was applied to optimize the objective functions, including the motor losses and material costs. The optimization process of the GA technique can be seen in Figure 1 in [14]. The process begins by defining the initial parameters, including the optimization variables and constraints. These optimization variables and constraints define the search space for the GA. With the predefined objective functions, the optimization variables and constraints are applied to calculate the values of the objective functions. Each set of optimization parameter values is an individual in the first generation's population. For each individual, a set of results is obtained for the objective functions. These objective function results are then compared with the evaluation criteria. If the criteria to stop the loop are not met, the next generation is created by randomly selecting individuals from the first generation's population. These individuals are then input into the algorithm to compute the objective function values using methods such as reproduction, crossover, and mutation. After the calculation process, the objective function results are compared with the evaluation criteria. If the stopping conditions are not met, a new iteration is carried out as described above, or else the best result sets are presented through the Pareto chart, and the optimization process concludes. In this study, 10 optimization variables were selected and included in the optimization process with the limits shown in Table II. Constraints are an essential part of the calculation process in any optimization method, as they limit the search space of the GA. There are two types of constraint functions: equality constraints and inequality constraints. This study applied inequality constraints to the volume of the stator, the rotor volume, and the magnet volume. Meanwhile, equality constraints were applied to the flux density limits on the stator core, rotor core, and stator teeth. Additionally, the slot filling factor was also limited within an empirical range according to motor manufacturers, from 0.35 to 0.55. Thus, the optimization problem includes three equality constraints and four inequality constraints:

- Equality constraints: Volume of the stator (V_{stator}) = constant, volume of the rotor (V_{rotor}) = constant, and volume of the PM: (V_{magnet}) = constant.
- Inequality constraints:
  - Magnetic flux density in the stator core: 1T≤B_{sy}≤1.5T
  - Magnetic flux density in the rotor core: 1T≤B_{sy}≤1.5T
  - Magnetic flux density in the teeth: 1.5T≤B_{tooth}≤2T
  - Slot filling factor: 0.35≤k_{fill}≤0.55.

TABLE II. BOUNDARY VALUES OF THE OPTIMIZATION VARIABLES.

Value	Lower boundary value	Upper boundary value
z_1 (mm): length of the air gap	0.6	0.8
z_2 (mm): inner stator diameter	145	155
z_3 (mm): thickness of the PM	1.5	2.5
z_4 (mm): stator core height	11	15
z_5: the magnitude of the V-angle	110	125
z_6: bridge length	1.2	2
z_7 (A/mm^2)	4.7	5.5
z_8 (turns)	28	34
z_9: (mm): tooth width	12	16
z_{10}: (mm): rotor core height	1.5	2.8

Objective functions are an essential part of any optimization method because they define the results to be obtained after the optimization process. Two objective functions were defined: total losses and material costs. The goal of the optimization method is to reduce both power losses and material costs. The material costs include the costs of magnetic steel, copper, and magnets, as expressed below [14]:

$$C = c_{Fe}M_{Fe} + c_{Cu}M_{Cu} + c_mM_m = c_{Fe}(M_s + M_r + M_t) + c_{Cu}M_{Cu} + c_mM_m \quad (9)$$

where c_{Fe}, c_{Cu}, c_m are the costs of magnetic steel, copper, and magnets, respectively. The expressions for M_s, M_r, M_t và M_m are as follows [14]:

$$M_s = A_1.(z_2 - 2z_1)^2.\left(\frac{V_s(z_2-2z_1)^2}{V_r} - {z_2}^2\right) \quad (10)$$

$$M_r = A_1.(z_2 - 2z_1)^2.\left(\left((z_2 - 2z_1)^2 - (z_2 - 2z_1 - 2\left((z_6 + \frac{V_m}{z_3.\overline{\pi.(z_2-2z_1)^2}}.Cos\frac{z_5}{2} + \left(\frac{z_2-2z_1}{2} - z_6\right).\left(1 - Cos\frac{A_3}{2}\right) + \frac{z_3}{Sin\frac{z_5}{2}}\right) + z_{10}\right)\right)^2\right) - \frac{4}{\pi}.A_2.z_3\right) \quad (11)$$

$$M_t = A_1.(z_2 - 2z_1)^2.\left(\left(\sqrt{\frac{V_s.(z_2-2z_1)^2}{V_r}} - 2z_4\right)^2 - {z_1}^2\right) - \frac{4A_1.(z_2-2z_1)^2}{\pi}Q_s.A_4 \quad (12)$$

$$M_{Cu} = \frac{8960.I.Q_s.L_{dq}}{z_7.10^{-6}};\ M_m = V_m.4p.7500 \quad (13)$$

The factors from A_1 to A_4 are calculated as follows:

$$A_1 = V_r.7650.10^{-9};\quad A_2 = w_m.4p \quad (14)$$

$$A_3 = 2.\text{asin}\left(\left(\frac{V_m}{z_3.\overline{\pi.(z_2-2z_1)^2}} + 2\right).\frac{Sin\frac{z_5}{2}}{\frac{z_2-2z_1}{2} - z_6}\right) \quad (15)$$

$$A_4 = b_{s1}.(h_s + h_{s0} + 2h_w) + b_{s2}.(h_s + h_{s0} + h_w) + b_{s0}.(h_w + 2h_{s0}) \quad (16)$$

where the parameters $V_s, V_r, V_m, B_r, B_m, h_w, h_{so}, b_{so}$ are the volumes of the stator, rotor, and magnet, along with the residual magnetic flux density of the magnet at ambient temperature, the operating magnetic flux density of the magnet, the wedge height, the slot mouth depth, and the slot mouth width.

The total losses in the IPM include core losses and copper losses, expressed as follows [14]:

$$P_{loss} = p_s M_s + p_r M_r + p_t M_t + N_s I^2 R \quad (17)$$

where N_s is the number of slots, I is the phase current, R is the winding resistance per tooth, M_s is the mass of the stator core, M_r is the mass of the rotor core, and M_t is the mass of stator teeth.

The loss per kilogram of the stator core (p_s) is calculated as [14]:

$$p_s = k_h.f.\left(\frac{B_g.\pi}{8p}\right)^{1.7}.\left(\frac{2z_2-2z_1}{z_4}\right)^{1.7} + k_e.f^2.(\frac{B_g.\pi}{8p})^2.(\frac{2z_2-2z_1}{z_4})^2 \quad (18)$$

The loss per kilogram of the rotor core (p_r) has already been given [14]. The loss per kilogram of the stator teeth (p_t) is calculated as:

$$p_t = k_h.f.\left(\frac{B_g.\pi}{N_s}\right)^{1.7}.\left(\frac{z_2-z_1}{z_9}\right)^{1.7} + k_e.f^2.(\frac{B_g.\pi}{N_s})^2.(\frac{z_2-z_1}{z_9})^2 \quad (19)$$

The resistance (R) of each coil winding on a tooth:

$$R = \frac{\rho_{Cu}.L_{dq}.z_7}{I.10^{-6}} \quad (20)$$

L_{dq} is the length of the coil winding on each tooth, determined as:

$$L_{dq} = (z_9 + \frac{4V_r}{\pi.(z_2-2z_1)^2} + ceil\left(\frac{z_8}{floor\left(\sqrt{\frac{(4h_s{}^2+(b_{s2}-b_{s1})^2).I_{n.1,15}}{\pi}}.\frac{1}{z_7}\right)}\right).\sqrt{\frac{4.I_{n.1,15}}{\pi}}.\frac{1}{z_7}).2.z_8 \quad (21)$$

IV. NUMERICAL TEST

Based on the input parameters given in Table I, the test was first carried out with the analytical technique to define the required/main parameters of 7.5 kW, voltage of 400 V, f=125 Hz. Figure 2 shows the Pareto front results. It can be observed that the two objective functions, material cost and total losses, exhibit an inverse relationship: As the material cost decreases, the losses increase and vice versa. This study chose a weight of 0.3 for total losses and a weight of 0.7 for material cost to determine the point with the minimum value for the sum of both objective functions to calculate the motor parameters after optimization. Figure 3 shows the magnetic flux density distribution in the stator and rotor before and after optimization.

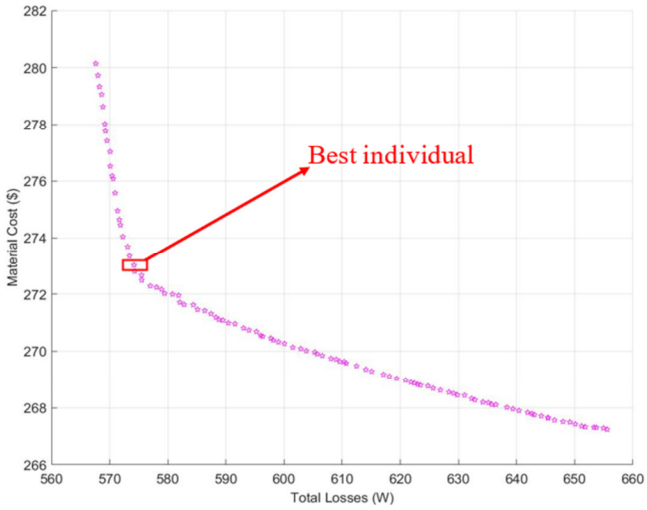

Fig. 2. Pareto front optimization results.

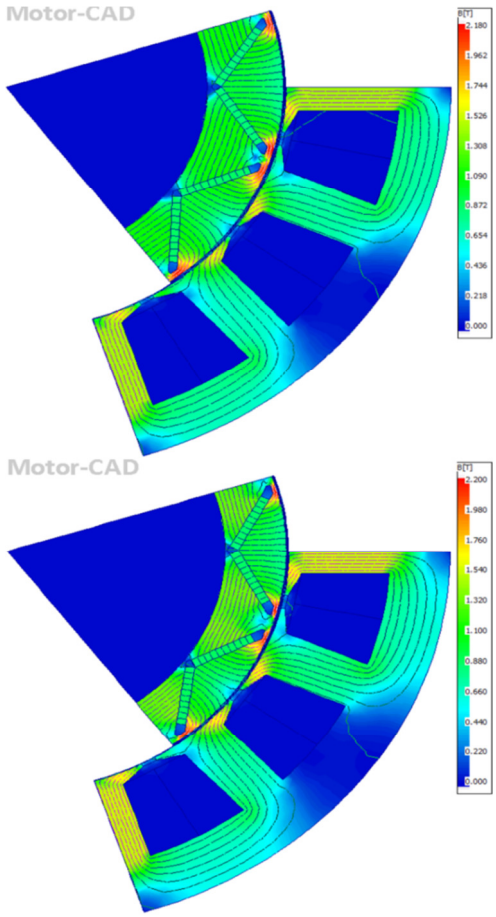

Fig. 3. Magnetic flux density distribution in the stator and rotor before (top) and after (bottom) optimization.

It can be observed that, before optimization, the maximum magnetic flux density value is 2.18 T at the Bridge position. After optimization, the maximum value is 2.2 T at the same position. This means that the maximum magnetic flux density in the air gap was increased by 0.02 T. This value is small and insignificant and is not likely to cause saturation of the magnetic circuit. Figure 4 shows the distribution of the magnetic flux density in the air gap before and after optimization. Figure 5 shows the waveform of the back EMF. Figure 6 shows the reduction in THD (Total Harmonic Distortion) of the back EMF in the motor, from 5.7% to 3%. The THD of the back EMF was significantly decreased, due to the significant reduction in the large-value harmonic components at the 1st, 5th, and 11th orders. It can be seen that the torque on the motor shaft increased after the optimization process, from 47.77 Nm to 48.21 Nm. This is also due to the drop in THD of the back EMF. Figure 7 shows the distribution of the cogging torque in both cases (before and after optimization). The value after optimization slightly increased compared to before optimization because the air gap size of the motor was reduced after optimization.

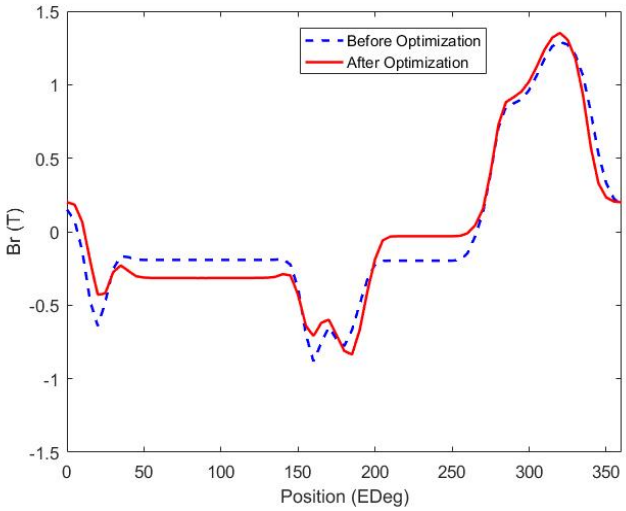

Fig. 4. Radial magnetic flux distribution.

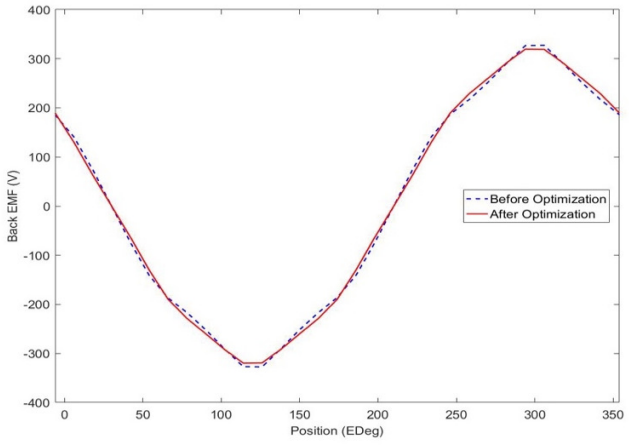

Fig. 5. Waveform of back EMF.

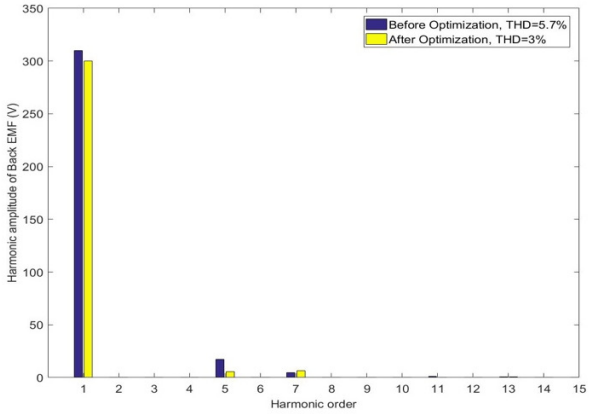

Fig. 6. Harmonic amplitude in the Back EMF.

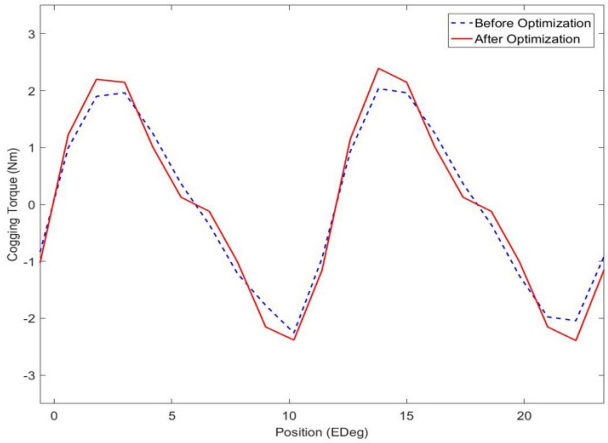

Fig. 7. Waveform distribution of cogging torque.

Figure 8 shows that torque quality improved significantly. Torque ripple is the fluctuation of the torque, shown in Figure 9. The torque ripple of the motor after optimization was 3.65%, much lower than the 12.86% before optimization. Therefore, the torque quality improved, while the efficiency of the machine increased from 95.44% before optimization to 95.77% after optimization. These are expected results, confirming the effectiveness of the optimization method applied in this study.

Table III shows the optimization results for the main parameters of the IPM. The optimization process yielded favorable results, as the percentage of torque ripples decreased, while the motor efficiency increased. The power factor has a significant impact on motor operation. If this value is high, it reduces energy losses and the heat generated in the motor, thus increasing the motor's lifespan. As expected, the power factor also improved significantly from 0.9 to 0.95. Furthermore, the output torque demonstrated more stable performance after optimization, indicating a significant reduction in torque ripple. Although there is a slight increase in flux density on the teeth, it is not large enough to cause magnetic saturation and does not affect any motor parameters during operation. These favorable results emphasize the advantageous comparison between the optimized design and the initial configuration, as shown in Table IV.

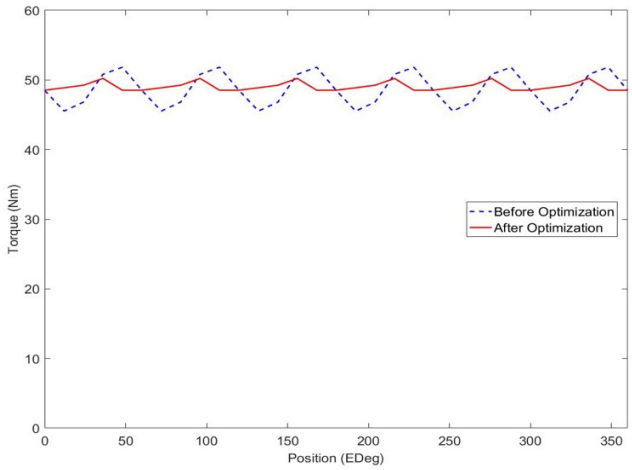

Fig. 8. Distribution of torque waveform.

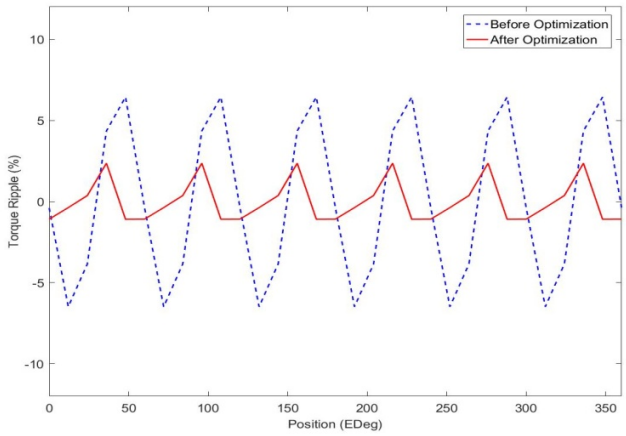

Fig. 9. Waveform of torque ripple.

TABLE III. MAIN DIMENSIONAL PARAMETERS BEFORE AND AFTER OPTIMIZATION

Quantity	Before optimization	After optimization
Outer stator diameter (mm)	240.53	231.8
Inner rotor diameter (mm)	108.77	113.77
Tooth width (mm)	14.46	13.8
Slot height (mm)	30.6	26.5
Magnet thickness (mm)	2.3	2.5
V-angle (electrical degrees)	114	124
Number of turns	29	27
Conductor diameter (mm)	2.714	2.76

TABLE IV. ELECTROMAGNETIC PARAMETERS BEFORE AND AFTER OPTIMIZATION

Quantity	Before optimization	After optimization
Output power (W)	7503.6	7573
Back EMF (V)	126.8	127
Efficiency (%)	95.44	95.77
Cogging torque (Nm)	4.3	4.7
Torque Ripple (%)	12.87	3.65
Power factor	0.9	0.95
Shaft torque (Nm)	47.77	48.21
Back EMF THD (%)	5.7	3
Bmax (T)	2.18	2.2
Cost ($)	279.9	272.8

V. CONCLUSION

This study examined a practical motor by performing analytical calculations and utilizing a GA to optimize losses and material costs. The parameters of a 7.5 kW IPM motor were calculated and optimized based on the GA technique with 10 variables. The primary objective of the optimization process was to minimize total losses and material costs, which are two critical factors. FEM was applied to evaluate the performance of the motor and determine the influence of the selected variables and constraints during the optimization process. The results demonstrated that the optimized design not only reduced material costs compared to the original design while maintaining the desired performance level, but also yielded favorable improvements in other parameters such as flux density, torque ripple, and cogging torque. Future studies could explore the impact of further optimizations on motor lifespan and performance under varying environmental conditions. Additionally, further research could focus on the integration of these optimized motors into smart grid systems and renewable energy technologies to promote sustainability.

ACKNOWLEDGMENT

This research was funded by the Hanoi University of Science and Technology (HUST) under project number T2024-PC-060.

REFERENCES

[1] L. Feng, S. Yu, F. Zhang, S. Jin, and Y. Sun, "Study on performance of low-speed high-torque permanent magnet synchronous motor with dynamic eccentricity rotor," *Energy Reports*, vol. 8, pp. 1421–1428, Aug. 2022, https://doi.org/10.1016/j.egyr.2022.03.018.

[2] J. M. Crider and S. D. Sudhoff, "An Inner Rotor Flux-Modulated Permanent Magnet Synchronous Machine for Low-Speed High-Torque Applications," *IEEE Transactions on Energy Conversion*, vol. 30, no. 3, pp. 1247–1254, Sep. 2015, https://doi.org/10.1109/TEC.2015.2412547.

[3] L. Qinghua, "Analysis, design and control of permanent magnet synchronous motors for wide-speed operation," Ph.D. dissertation, National University of Singapore, 2005.

[4] M. Sundaram *et al.*, "Design and FEM Analysis of High-Torque Power Density Permanent Magnet Synchronous Motor (PMSM) for Two-Wheeler E-Vehicle Applications," *International Transactions on Electrical Energy Systems*, vol. 2022, pp. 1–14, Jul. 2022, https://doi.org/10.1155/2022/1217250.

[5] E. Tun and T. Tin, "Design of conventional permanent magnet synchronous motor used in electric vehicle," *International Journal of Scientific Engineering and Technology Research*, vol. 3, no. 16, pp. 3289–3293, 2014.

[6] G. Liu, M. Liu, Y. Zhang, H. Wang, and C. Gerada, "High-Speed Permanent Magnet Synchronous Motor Iron Loss Calculation Method Considering Multiphysics Factors," *IEEE Transactions on Industrial Electronics*, vol. 67, no. 7, pp. 5360–5368, Jul. 2020, https://doi.org/10.1109/TIE.2019.2934075.

[7] Y. Gao, T. Yang, S. Bozhko, P. Wheeler, T. Dragicevic, and C. Gerada, "Neural Network aided PMSM multi-objective design and optimization for more-electric aircraft applications," *Chinese Journal of Aeronautics*, vol. 35, no. 10, pp. 233–246, Oct. 2022, https://doi.org/10.1016/j.cja.2021.08.006.

[8] W. A. Pluta, "Core loss models in electrical steel sheets with different orientation," *Przegląd Elektrotechniczny*, vol. 87, pp. 37–42, 2011.

[9] S. Mishra and S. Sahoo, "Genetic Algorithm: An Efficient Tool for Global Optimization," *Advances in Computational Sciences and Technology*, vol. 10, no. 8, pp. 2201–2211, 2017.

[10] G. Cvetkovski and L. Petkovska, "Multi-objective optimal design of permanent magnet synchronous motor," in *2016 IEEE International*

Power Electronics and Motion Control Conference (PEMC), Varna, Bulgaria, Sep. 2016, pp. 605–610, https://doi.org/10.1109/EPEPEMC.2016.7752064.

[11] J. Gao, L. Dai, and W. Zhang, "Improved genetic optimization algorithm with subdomain model for multi-objective optimal design of SPMSM," *CES Transactions on Electrical Machines and Systems*, vol. 2, no. 1, pp. 160–165, Mar. 2018, https://doi.org/10.23919/TEMS.2018.8326463.

[12] C. C. Hwang, L. Y. Lyu, C. T. Liu, and P. L. Li, "Optimal Design of an SPM Motor Using Genetic Algorithms and Taguchi Method," *IEEE Transactions on Magnetics*, vol. 44, no. 11, pp. 4325–4328, Nov. 2008, https://doi.org/10.1109/TMAG.2008.2001526.

[13] W. Zhao, H. Shen, W. Chai, X. Wang, and B. Kwon, "Optimal Design and Experimental Test of a SPM Motor With Cost-Effective Magnet Utilization to Suppress Torque Pulsations," *IEEE Transactions on Magnetics*, vol. 54, no. 11, pp. 1–5, Nov. 2018, https://doi.org/10.1109/TMAG.2018.2842714.

[14] T. C. Truong, T. N. Vu, H. B. Duc, and V. D. Quoc, "Using Genetic Algorithms for Optimal Electromagnetic Parameters of SPM Synchronous Motors," *Journal Européen des Systèmes Automatisés*, vol. 56, no. 6, pp. 899–906, Dec. 2023, https://doi.org/10.18280/jesa.560601.

[15] P. Ngatchou, A. Zarei, and A. El-Sharkawi, "Pareto Multi Objective Optimization," in *Proceedings of the 13th International Conference on, Intelligent Systems Application to Power Systems*, Arlington, VA, USA, 2005, pp. 84–91, https://doi.org/10.1109/ISAP.2005.1599245.

[16] D. Q. Nguyen, T. N. Thai, C. L. Thi, D. B. Minh, and V. D. Quoc, "Association between the Analytical Technique and Finite Element Method for designing SPMSMs with Inner Rotor Type for Electric Vehicle Applications," *Engineering, Technology & Applied Science Research*, vol. 14, no. 3, pp. 14119–14124, Jun. 2024, https://doi.org/10.48084/etasr.7087.

[17] J. Pyrhönen, T. Jokinen, and V. Hrabovcová, *Design of Rotating Electrical Machines*, 1st ed. Wiley, 2013.

Electromagnetic Parameters of IPM Motors based on the Genetic Algorithm Technique

Quang Nguyen Duc
Faculty of Electrical Engineering, Electric Power University, Ha Noi, Vietnam
quangndhtd@epu.edu.vn

Thang Nguyen Duy
School of Electrical and Electronic Engineering, Hanoi University of Science and Technology, Vietnam
thang.nd210779@sis.hust.edu.vn

Trinh Truong Cong
School of Electrical and Electronic Engineering, Hanoi University of Science and Technology, Vietnam
trinh.truongcong@hust.edu.vn

Nam Le Hai
School of Electrical and Electronic Engineering, Hanoi University of Science and Technology, Vietnam
nam.lh210629@sis.hust.edu.vn

Duong Doan Le Quy
School of Electrical and Electronic Engineering, Hanoi University of Science and Technology, Vietnam
duong.dlq212493@sis.hust.edu.vn

Vuong Dang Quoc
School of Electrical and Electronic Engineering, Hanoi University of Science and Technology, Vietnam
vuong.dangquoc@hust.edu.vn

Dinh Bui Minh
School of Electrical and Electronic Engineering, Hanoi University of Science and Technology, Vietnam
dinh.buiminh@hust.edu.vn (corresponding author)

Received: 13 February 2025 | Revised: 21 March 2025 | Accepted: 2 April 2025

 DOI: https://doi.org/10.48084/etasr.10559

ABSTRACT

Interior Permanent Magnet Synchronous Motors (IPMSM) are increasingly utilized across various fields as a result of their superior performance and high power density. To ensure efficient operation in electric vehicles and industrial applications, these motors have to meet the stringent performance objectives of low vibration. This study proposes an optimization method based on Genetic Algorithm (GA) techniques to minimize losses and material costs. First, an analytical model is developed to determine the required parameters for an IPM motor with five pole pairs, 15 slots, and a power rating of 7.5 kW. Subsequently, the GA is implemented using the analytical model to optimize the electromagnetic parameters of the IPM motor. Finally, the Finite Element Method (FEM) is applied to simulate the parameters obtained from the analytical model and GA. The results before and after optimization, including material cost functions, total losses, and motor outputs, were compared to validate the proposed method.

Keywords-Interior Permanent Magnet Synchronous Motor (IPMSM); GA; cogging torque; torque ripple; analytical model

I. INTRODUCTION

Due to their high power density, efficiency, stable operation, and reliability, the Permanent Magnet Synchronous Motors (PMSMs) have been widely applied in industrial fields and electric vehicles in recent years [1-6]. PMSMs have contributed significantly to technological advancements and the creation of more energy-efficient systems by using permanent magnet materials such as neodymium-iron-boron (NdFeB) and samarium-cobalt (SmCo) [7]. In [8, 9], the Genetic Algorithm (GA) was used to optimize the main parameters of the motor. This technique has been employed in numerous studies to analyze optimal PMSM designs [10-13]. In [10], a multi-objective optimization design was developed for PMSMs using the artificial bee colony algorithm, achieving high dynamic performance and overall efficiency of 94.5% to 96%. In [11], a subdomain model was combined with GA to optimize the design of Surface-mounted PMSMs (SPMSMs). This study used a subdomain model to accurately evaluate the flux density harmonics. Next, a Pareto-optimal set of solutions was searched with the subdomain model, allowing time savings. Finally, the electromagnetic performance of the new design was verified using FEM and compared with the original design and the traditionally GA-optimized design. In [12], the GA technique was utilized in conjunction with Taguchi optimization and FEM to calculate the performance of SPMSMs. The results indicated that a reduction in the cogging torque results in a small reduction of efficiency from GAs to Taguchi design due to the reduction of magnet volume. In [13], an improved SPMSM design was proposed to reduce torque pulsations and save magnet costs. In [14, 15], a partitioned model was combined with GA to achieve an optimal SPMSM design. In this study, the partitioned model was developed in advance to accurately assess the flux density. Then, a Pareto-optimal set of solutions was obtained by applying the GA technique.

In this context, this study uses the GA technique to improve the electromagnetic parameters of IPM motors. First, an analytical model is provided to define the parameters required for motor design. Then, an optimization model based on the GA technique is developed to optimize the material cost and losses of the motor. Finally, FEM is applied to perform simulations and compare the results of the electromagnetic parameters of the proposed motor before and after optimization.

II. ANALYTICAL BACKGROUND

Figure 1 provides the analytical design steps of the PMSM. The volume (V_r) of the rotor is defined via the torque density (TRV) [16]:

$$V_r = \frac{\pi}{4}.{D_{is}}^2.L = \frac{T}{TRV} \quad (1)$$

where T is the electromagnetic torque, D_{is} is the inner diameter of the stator, and L is the length of the rotor.

The TRV value is selected from 35 kNm/m^3 to 85 kNm/m^3 [16]. The stator can be calculated similarly to the stator of an asynchronous motor, using the following formulas [16]:

$$D_{is} = \sqrt[3]{\frac{4V_r}{\pi.k_{shape}}} \quad (2)$$

where k_{shape} is the shape factor given in [16]. The thickness of the magnet is determined by:

$$d_m = \frac{\mu_r.geffB_g}{4B_r \sin(\alpha) - B_g\pi} \quad (3)$$

where B_r is the PM remanence, g_{eff} is the effective air gap length, μ_r is the relative permeability of the PM, and B_g is the magnetic flux density in the air gap. The B_g vallue can be selected from 0.8 T to 1.05 T [16]. The width of the magnet is determined by:

$$w_m = \frac{A_m}{L} \quad (4)$$

The PM opening angle in electrical degrees is computed as:

$$\beta = 2p.\arcsin\left[w_m.\left(\frac{\alpha_V}{D_{or}-2x_1}\right)\right] \quad (5)$$

The depth (d_p) of a V-shape pole (α_V) is given by:

$$d_p = x_1 + w_m.cos\left(\frac{\alpha_V}{2}\right) + \left(\frac{D_{or}}{2} - x_1\right)\left[1 - cos\left(\frac{\beta}{2}\right)\right] + \frac{d_m}{sin\left(\frac{\alpha_V}{2}\right)} \quad (6)$$

where w_m is the width of the PM. The height of the rotor yoke and the number of turns are represented below:

$$h_{ry} = \frac{\phi_g}{2.B_{ry}.L.k_j} - d_p;\ N_c = \frac{U_{phase}}{\pi\sqrt{2}fk_wB_gD_{ir}L} \quad (7)$$

The parameters h_{sy} and w_t have been already defined in [17]. The V-angle of the magnet and the magnitude of the bridge length in the IPM motor can also be adjusted depending on the design to suit the requirements.

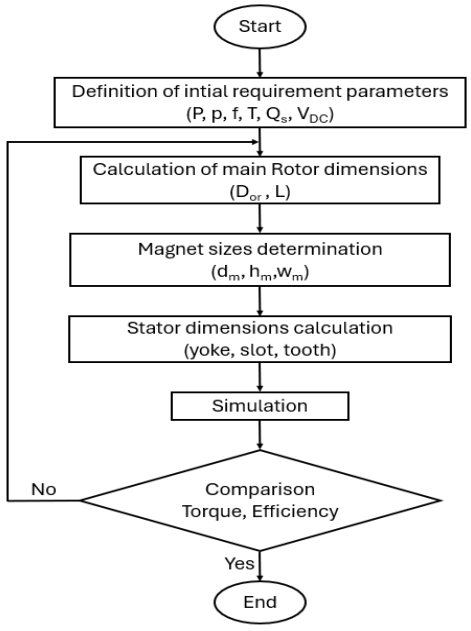

Fig. 1. Design steps of PMSM.

TABLE I. COMPUTATIONAL PARAMETERS OF THE 7.5KW IPM MOTOR

Parameters	Values	Unit
Number of slots	15	
Number of poles	10	
Inner diameter of stator	151.45	mm
Outer diameter of stator	240.53	mm
Tooth width	14.46	mm
Slot height	30.6	mm
Air gap length	0.8	mm
Inner diameter of rotor	108.77	mm
Magnet thickness	2.3	mm
Magnet width	20.4	mm
Bridge length	2	mm
V-angle	114	Elec degrees
Electrical angle of the magnet	149.3	Elec degrees
Number of turns	29	

III. GA TECHNIQUE FOR PARAMETER OPTIMIZATION

GA was applied to optimize the objective functions, including the motor losses and material costs. The optimization process of the GA technique can be seen in Figure 1 in [14]. The process begins by defining the initial parameters, including the optimization variables and constraints. These optimization variables and constraints define the search space for the GA. With the predefined objective functions, the optimization variables and constraints are applied to calculate the values of the objective functions. Each set of optimization parameter values is an individual in the first generation's population. For each individual, a set of results is obtained for the objective functions. These objective function results are then compared with the evaluation criteria. If the criteria to stop the loop are not met, the next generation is created by randomly selecting individuals from the first generation's population. These individuals are then input into the algorithm to compute the objective function values using methods such as reproduction, crossover, and mutation. After the calculation process, the objective function results are compared with the evaluation criteria. If the stopping conditions are not met, a new iteration is carried out as described above, or else the best result sets are presented through the Pareto chart, and the optimization process concludes. In this study, 10 optimization variables were selected and included in the optimization process with the limits shown in Table II. Constraints are an essential part of the calculation process in any optimization method, as they limit the search space of the GA. There are two types of constraint functions: equality constraints and inequality constraints. This study applied inequality constraints to the volume of the stator, the rotor volume, and the magnet volume. Meanwhile, equality constraints were applied to the flux density limits on the stator core, rotor core, and stator teeth. Additionally, the slot filling factor was also limited within an empirical range according to motor manufacturers, from 0.35 to 0.55. Thus, the optimization problem includes three equality constraints and four inequality constraints:

- Equality constraints: Volume of the stator (V_{stator}) = constant, volume of the rotor (V_{rotor}) = constant, and volume of the PM: (V_{magnet}) = constant.
- Inequality constraints:
  - Magnetic flux density in the stator core: 1T≤B_{sy}≤1.5T
  - Magnetic flux density in the rotor core: 1T≤B_{sy}≤1.5T
  - Magnetic flux density in the teeth: 1.5T≤B_{tooth}≤2T
  - Slot filling factor: 0.35≤k_{fill}≤0.55.

TABLE II. BOUNDARY VALUES OF THE OPTIMIZATION VARIABLES.

Value	Lower boundary value	Upper boundary value
z_1 (mm): length of the air gap	0.6	0.8
z_2 (mm): inner stator diameter	145	155
z_3 (mm): thickness of the PM	1.5	2.5
z_4 (mm): stator core height	11	15
z_5: the magnitude of the V-angle	110	125
z_6: bridge length	1.2	2
z_7 (A/mm^2)	4.7	5.5
z_8 (turns)	28	34
z_9: (mm): tooth width	12	16
z_{10}: (mm): rotor core height	1.5	2.8

Objective functions are an essential part of any optimization method because they define the results to be obtained after the optimization process. Two objective functions were defined: total losses and material costs. The goal of the optimization method is to reduce both power losses and material costs. The material costs include the costs of magnetic steel, copper, and magnets, as expressed below [14]:

$$C = c_{Fe}M_{Fe} + c_{Cu}M_{Cu} + c_mM_m = c_{Fe}(M_s + M_r + M_t) + c_{Cu}M_{Cu} + c_mM_m \quad (8)$$

where c_{Fe}, c_{Cu}, c_m are the costs of magnetic steel, copper, and magnets, respectively. The expressions for M_s, M_r, M_t và M_m are as follows [14]:

$$M_s = A_1.(z_2 - 2z_1)^2.\left(\frac{V_s(z_2-2z_1)^2}{V_r} - {z_2}^2\right) \quad (9)$$

$$M_r = A_1.(z_2 - 2z_1)^2.\left(\left((z_2 - 2z_1)^2 - (z_2 - 2z_1 - 2\left(\left(z_6 + \frac{V_m}{z_3.\overline{\pi.(z_2-2z_1)^2}}\right).Cos\frac{z_5}{2} + \left(\frac{z_2-2z_1}{2} - z_6\right).\left(1 - Cos\frac{A_3}{2}\right) + \frac{z_3}{Sin\frac{z_5}{2}}\right) + z_{10}\right)\right)^2\right) - \frac{4}{\pi}.A_2.z_3) \quad (10)$$

$$M_t = A_1.(z_2 - 2z_1)^2.\left(\left(\sqrt{\frac{V_s.(z_2-2z_1)^2}{V_r}} - 2z_4\right)^2 - {z_1}^2\right) - \frac{4A_1.(z_2-2z_1)^2}{\pi}Q_s.A_4 \quad (11)$$

$$M_{Cu} = \frac{8960.I.Q_s.L_{dq}}{z_7.10^{-6}};\ M_m = V_m.4p.7500 \quad (12)$$

The factors from A_1 to A_4 are calculated as follows:

$$A_1 = V_r.7650.10^{-9};\quad A_2 = w_m.4p \quad (13)$$

$$A_3 = 2.\text{asin}\left(\left(\frac{V_m}{z_3.\overline{\pi.(z_2-2z_1)^2}} + 2\right).\frac{Sin\frac{z_5}{2}}{\frac{z_2-2z_1}{2} - z_6}\right) \quad (14)$$

$$A_4 = b_{s1}.(h_s + h_{s0} + 2h_w) + b_{s2}.(h_s + h_{s0} + h_w) + b_{s0}.(h_w + 2h_{s0}) \quad (15)$$

where the parameters $V_s, V_r, V_m, B_r, B_m, h_w, h_{so}, b_{so}$ are the volumes of the stator, rotor, and magnet, along with the residual magnetic flux density of the magnet at ambient temperature, the operating magnetic flux density of the magnet, the wedge height, the slot mouth depth, and the slot mouth width.

The total losses in the IPM include core losses and copper losses, expressed as follows [14]:

$$P_{loss} = p_s M_s + p_r M_r + p_t M_t + N_s I^2 R \quad (16)$$

where N_s is the number of slots, I is the phase current, R is the winding resistance per tooth, M_s is the mass of the stator core, M_r is the mass of the rotor core, and M_t is the mass of stator teeth.

The loss per kilogram of the stator core (p_s) is calculated as [14]:

$$p_s = k_h.f.\left(\frac{B_g.\pi}{8p}\right)^{1.7}.\left(\frac{2z_2-2z_1}{z_4}\right)^{1.7} + k_e.f^2.(\frac{B_g.\pi}{8p})^2.(\frac{2z_2-2z_1}{z_4})^2 \quad (17)$$

The loss per kilogram of the rotor core (p_r) has already been given [14]. The loss per kilogram of the stator teeth (p_t) is calculated as:

$$p_t = k_h.f.\left(\frac{B_g.\pi}{N_s}\right)^{1.7}.\left(\frac{z_2-z_1}{z_9}\right)^{1.7} + k_e.f^2.(\frac{B_g.\pi}{N_s})^2.(\frac{z_2-z_1}{z_9})^2 \quad (18)$$

The resistance (R) of each coil winding on a tooth:

$$R = \frac{\rho_{Cu}.L_{dq}.z_7}{I.10^{-6}} \quad (19)$$

L_{dq} is the length of the coil winding on each tooth, determined as:

$$L_{dq} = (z_9 + \frac{4V_r}{\pi.(z_2-2z_1)^2} + ceil\left(\frac{z_8}{floor\left(\sqrt{\frac{(4h_s{}^2+(b_{s2}-b_{s1})^2).I_{n.1,15}}{\pi}}.\frac{1}{z_7}\right)}\right).\sqrt{\frac{4.I_{n.1,15}}{\pi}}.\frac{1}{z_7}).2.z_8 \quad (20)$$

IV. NUMERICAL TEST

Based on the input parameters given in Table I, the test was first carried out with the analytical technique to define the required/main parameters of 7.5 kW, voltage of 400 V, f=125 Hz. Figure 2 shows the Pareto front results. It can be observed that the two objective functions, material cost and total losses, exhibit an inverse relationship: As the material cost decreases, the losses increase and vice versa. This study chose a weight of 0.3 for total losses and a weight of 0.7 for material cost to determine the point with the minimum value for the sum of both objective functions to calculate the motor parameters after optimization. Figure 3 shows the magnetic flux density distribution in the stator and rotor before and after optimization.

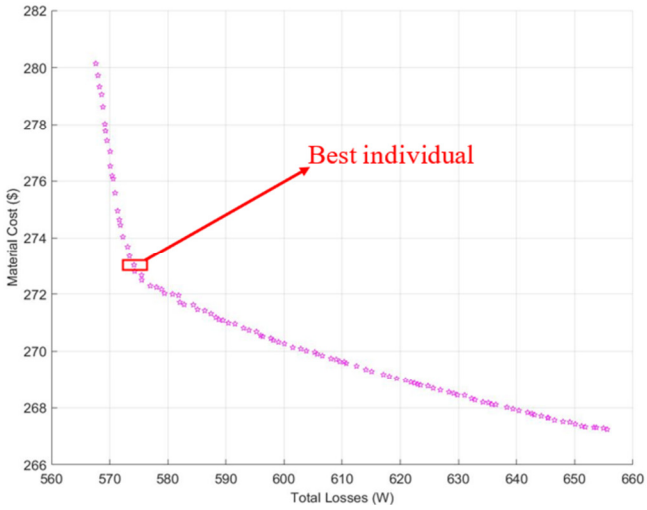

Fig. 2. Pareto front optimization results.

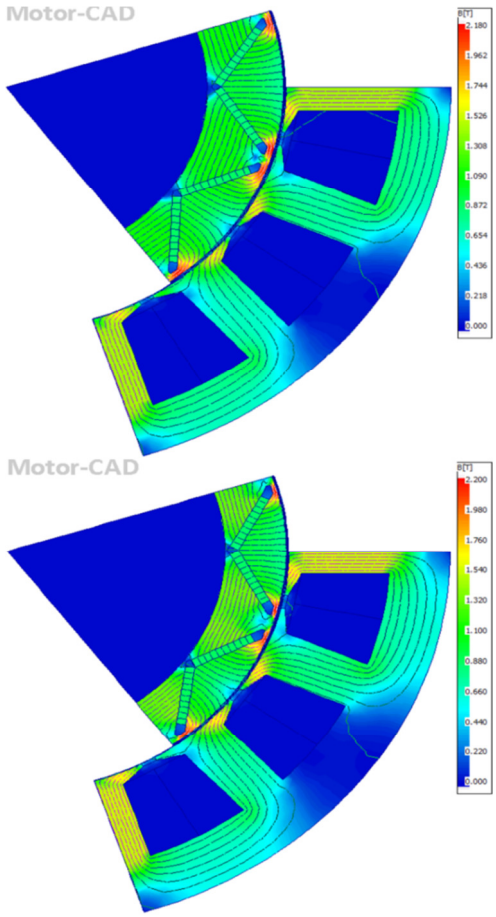

Fig. 3. Magnetic flux density distribution in the stator and rotor before (top) and after (bottom) optimization.

It can be observed that, before optimization, the maximum magnetic flux density value is 2.18 T at the Bridge position. After optimization, the maximum value is 2.2 T at the same position. This means that the maximum magnetic flux density in the air gap was increased by 0.02 T. This value is small and insignificant and is not likely to cause saturation of the magnetic circuit. Figure 4 shows the distribution of the magnetic flux density in the air gap before and after optimization. Figure 5 shows the waveform of the back EMF. Figure 6 shows the reduction in THD (Total Harmonic Distortion) of the back EMF in the motor, from 5.7% to 3%. The THD of the back EMF was significantly decreased, due to the significant reduction in the large-value harmonic components at the 1st, 5th, and 11th orders. It can be seen that the torque on the motor shaft increased after the optimization process, from 47.77 Nm to 48.21 Nm. This is also due to the drop in THD of the back EMF. Figure 7 shows the distribution of the cogging torque in both cases (before and after optimization). The value after optimization slightly increased compared to before optimization because the air gap size of the motor was reduced after optimization.

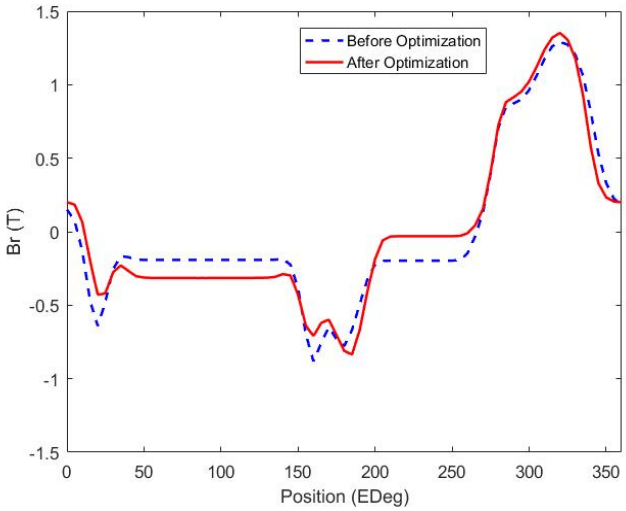

Fig. 4. Radial magnetic flux distribution.

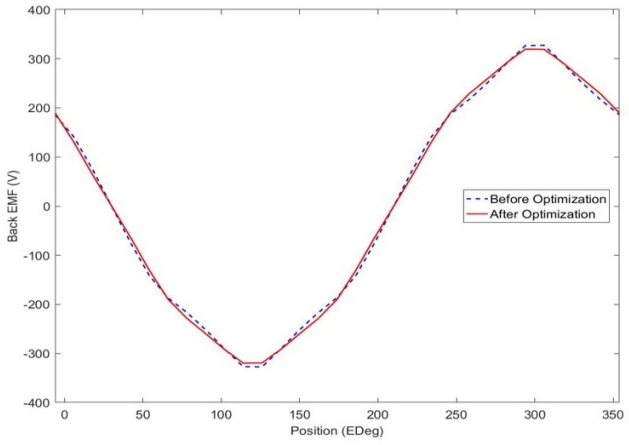

Fig. 5. Waveform of back EMF.

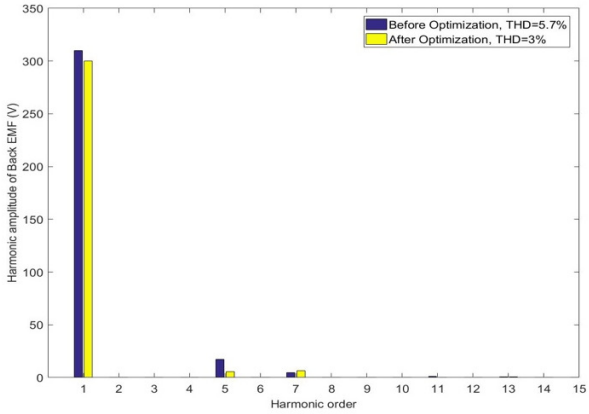

Fig. 6. Harmonic amplitude in the Back EMF.

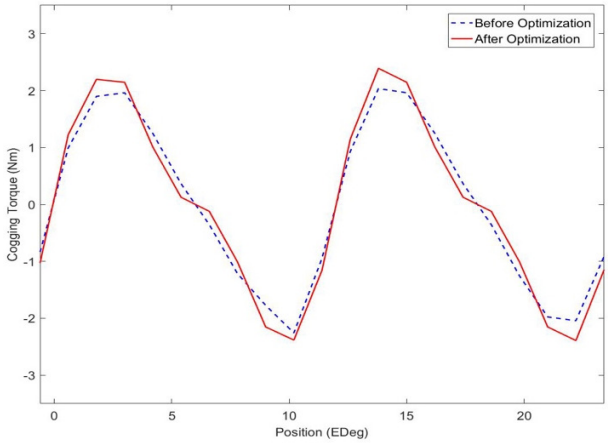

Fig. 7. Waveform distribution of cogging torque.

Figure 8 shows that torque quality improved significantly. Torque ripple is the fluctuation of the torque, shown in Figure 9. The torque ripple of the motor after optimization was 3.65%, much lower than the 12.86% before optimization. Therefore, the torque quality improved, while the efficiency of the machine increased from 95.44% before optimization to 95.77% after optimization. These are expected results, confirming the effectiveness of the optimization method applied in this study.

Table III shows the optimization results for the main parameters of the IPM. The optimization process yielded favorable results, as the percentage of torque ripples decreased, while the motor efficiency increased. The power factor has a significant impact on motor operation. If this value is high, it reduces energy losses and the heat generated in the motor, thus increasing the motor's lifespan. As expected, the power factor also improved significantly from 0.9 to 0.95. Furthermore, the output torque demonstrated more stable performance after optimization, indicating a significant reduction in torque ripple. Although there is a slight increase in flux density on the teeth, it is not large enough to cause magnetic saturation and does not affect any motor parameters during operation. These favorable results emphasize the advantageous comparison between the optimized design and the initial configuration, as shown in Table IV.

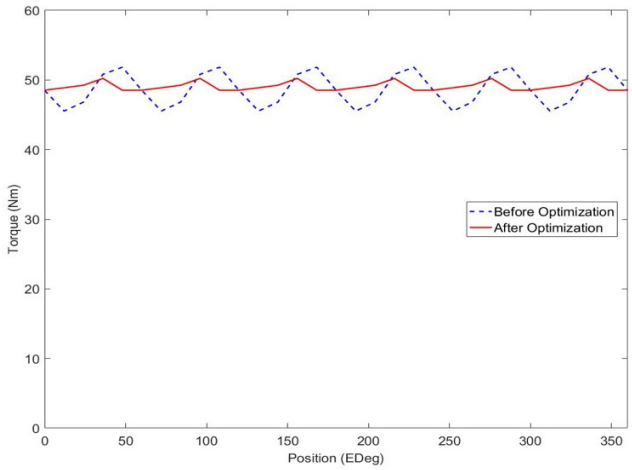

Fig. 8. Distribution of torque waveform.

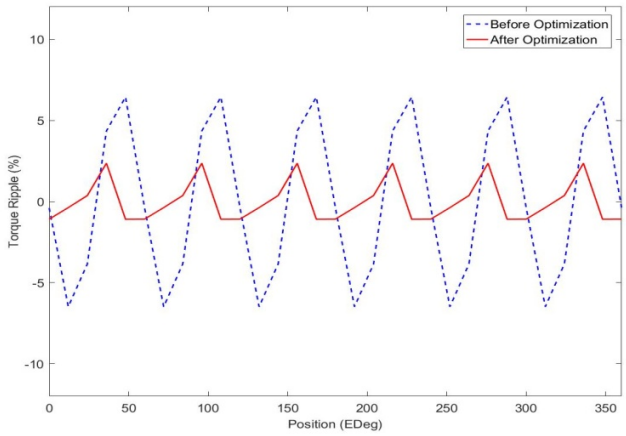

Fig. 9. Waveform of torque ripple.

TABLE III. MAIN DIMENSIONAL PARAMETERS BEFORE AND AFTER OPTIMIZATION

Quantity	Before optimization	After optimization
Outer stator diameter (mm)	240.53	231.8
Inner rotor diameter (mm)	108.77	113.77
Tooth width (mm)	14.46	13.8
Slot height (mm)	30.6	26.5
Magnet thickness (mm)	2.3	2.5
V-angle (electrical degrees)	114	124
Number of turns	29	27
Conductor diameter (mm)	2.714	2.76

TABLE IV. ELECTROMAGNETIC PARAMETERS BEFORE AND AFTER OPTIMIZATION

Quantity	Before optimization	After optimization
Output power (W)	7503.6	7573
Back EMF (V)	126.8	127
Efficiency (%)	95.44	95.77
Cogging torque (Nm)	4.3	4.7
Torque Ripple (%)	12.87	3.65
Power factor	0.9	0.95
Shaft torque (Nm)	47.77	48.21
Back EMF THD (%)	5.7	3
Bmax (T)	2.18	2.2
Cost ($)	279.9	272.8

V. CONCLUSION

This study examined a practical motor by performing analytical calculations and utilizing a GA to optimize losses and material costs. The parameters of a 7.5 kW IPM motor were calculated and optimized based on the GA technique with 10 variables. The primary objective of the optimization process was to minimize total losses and material costs, which are two critical factors. FEM was applied to evaluate the performance of the motor and determine the influence of the selected variables and constraints during the optimization process. The results demonstrated that the optimized design not only reduced material costs compared to the original design while maintaining the desired performance level, but also yielded favorable improvements in other parameters such as flux density, torque ripple, and cogging torque. Future studies could explore the impact of further optimizations on motor lifespan and performance under varying environmental conditions. Additionally, further research could focus on the integration of these optimized motors into smart grid systems and renewable energy technologies to promote sustainability.

ACKNOWLEDGMENT

This research was funded by the Hanoi University of Science and Technology (HUST) under project number T2024-PC-060.

REFERENCES

[1] L. Feng, S. Yu, F. Zhang, S. Jin, and Y. Sun, "Study on performance of low-speed high-torque permanent magnet synchronous motor with dynamic eccentricity rotor," *Energy Reports*, vol. 8, pp. 1421–1428, Aug. 2022, https://doi.org/10.1016/j.egyr.2022.03.018.

[2] J. M. Crider and S. D. Sudhoff, "An Inner Rotor Flux-Modulated Permanent Magnet Synchronous Machine for Low-Speed High-Torque Applications," *IEEE Transactions on Energy Conversion*, vol. 30, no. 3, pp. 1247–1254, Sep. 2015, https://doi.org/10.1109/TEC.2015.2412547.

[3] L. Qinghua, "Analysis, design and control of permanent magnet synchronous motors for wide-speed operation," Ph.D. dissertation, National University of Singapore, 2005.

[4] M. Sundaram *et al.*, "Design and FEM Analysis of High-Torque Power Density Permanent Magnet Synchronous Motor (PMSM) for Two-Wheeler E-Vehicle Applications," *International Transactions on Electrical Energy Systems*, vol. 2022, pp. 1–14, Jul. 2022, https://doi.org/10.1155/2022/1217250.

[5] E. Tun and T. Tin, "Design of conventional permanent magnet synchronous motor used in electric vehicle," *International Journal of Scientific Engineering and Technology Research*, vol. 3, no. 16, pp. 3289–3293, 2014.

[6] G. Liu, M. Liu, Y. Zhang, H. Wang, and C. Gerada, "High-Speed Permanent Magnet Synchronous Motor Iron Loss Calculation Method Considering Multiphysics Factors," *IEEE Transactions on Industrial Electronics*, vol. 67, no. 7, pp. 5360–5368, Jul. 2020, https://doi.org/10.1109/TIE.2019.2934075.

[7] Y. Gao, T. Yang, S. Bozhko, P. Wheeler, T. Dragicevic, and C. Gerada, "Neural Network aided PMSM multi-objective design and optimization for more-electric aircraft applications," *Chinese Journal of Aeronautics*, vol. 35, no. 10, pp. 233–246, Oct. 2022, https://doi.org/10.1016/j.cja.2021.08.006.

[8] W. A. Pluta, "Core loss models in electrical steel sheets with different orientation," *Przegląd Elektrotechniczny*, vol. 87, pp. 37–42, 2011.

[9] S. Mishra and S. Sahoo, "Genetic Algorithm: An Efficient Tool for Global Optimization," *Advances in Computational Sciences and Technology*, vol. 10, no. 8, pp. 2201–2211, 2017.

[10] G. Cvetkovski and L. Petkovska, "Multi-objective optimal design of permanent magnet synchronous motor," in *2016 IEEE International*

Power Electronics and Motion Control Conference (PEMC), Varna, Bulgaria, Sep. 2016, pp. 605–610, https://doi.org/10.1109/EPEPEMC.2016.7752064.

[11] J. Gao, L. Dai, and W. Zhang, "Improved genetic optimization algorithm with subdomain model for multi-objective optimal design of SPMSM," *CES Transactions on Electrical Machines and Systems*, vol. 2, no. 1, pp. 160–165, Mar. 2018, https://doi.org/10.23919/TEMS.2018.8326463.

[12] C. C. Hwang, L. Y. Lyu, C. T. Liu, and P. L. Li, "Optimal Design of an SPM Motor Using Genetic Algorithms and Taguchi Method," *IEEE Transactions on Magnetics*, vol. 44, no. 11, pp. 4325–4328, Nov. 2008, https://doi.org/10.1109/TMAG.2008.2001526.

[13] W. Zhao, H. Shen, W. Chai, X. Wang, and B. Kwon, "Optimal Design and Experimental Test of a SPM Motor With Cost-Effective Magnet Utilization to Suppress Torque Pulsations," *IEEE Transactions on Magnetics*, vol. 54, no. 11, pp. 1–5, Nov. 2018, https://doi.org/10.1109/TMAG.2018.2842714.

[14] T. C. Truong, T. N. Vu, H. B. Duc, and V. D. Quoc, "Using Genetic Algorithms for Optimal Electromagnetic Parameters of SPM Synchronous Motors," *Journal Européen des Systèmes Automatisés*, vol. 56, no. 6, pp. 899–906, Dec. 2023, https://doi.org/10.18280/jesa.560601.

[15] P. Ngatchou, A. Zarei, and A. El-Sharkawi, "Pareto Multi Objective Optimization," in *Proceedings of the 13th International Conference on, Intelligent Systems Application to Power Systems*, Arlington, VA, USA, 2005, pp. 84–91, https://doi.org/10.1109/ISAP.2005.1599245.

[16] D. Q. Nguyen, T. N. Thai, C. L. Thi, D. B. Minh, and V. D. Quoc, "Association between the Analytical Technique and Finite Element Method for designing SPMSMs with Inner Rotor Type for Electric Vehicle Applications," *Engineering, Technology & Applied Science Research*, vol. 14, no. 3, pp. 14119–14124, Jun. 2024, https://doi.org/10.48084/etasr.7087.

[17] J. Pyrhönen, T. Jokinen, and V. Hrabovcová, *Design of Rotating Electrical Machines*, 1st ed. Wiley, 2013.